Asian Journal of Chemistry; Vol. 35, No. 6 (2023), 1491-1499

ASIAN JOURNAL OF CHEMISTRY

https://doi.org/10.14233/ajchem.2023.27874

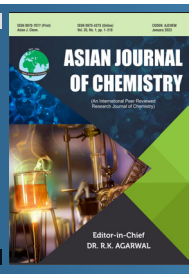


# Virtual Screening, DNA Strapping and Antimicrobial Investigation of Mixed Ligand Transition Metal Complexes

NAZEER MOHAMED NASAR[1], MICHAEL SAMUEL[1], PORKODI JAYARAMAN[2], FREEDA SELVA SHEELA[1] and NATARAJAN RAMAN[1,*]

[1]Research Department of Chemistry, VHNSN College (Autonomous) (Affiliated to Madurai Kamaraj University, Madurai), Virudhunagar-626001, India
[2]Post Graduate and Research Department of Chemistry, The Standard Fireworks Rajaratnam College for Women (Autonomous), Sivakasi-626123, India

*Corresponding author: Fax: +91 4562 281338; E-mail: ramchem1964@gmail.com

*Received*: 7 April 2023; *Accepted*: 8 May 2023; *Published online*: 27 May 2023; AJC-21268

To obtain the highest level of biological effectiveness, four transition metal *viz*., Cu(II), Zn(II), Co(II) and Ni(II) complexes *viz*. were synthesized using Schiff base obtained by the condensation reaction of *o*-phenylene diamine, 4-chlorobenzaldehyde and a co-ligand (malonic acid). Elemental analysis and other spectroscopic methods were used to identify them. All the synthesized metal(II) complexes have a square planar geometry, according to the physico-chemical analyses. The antibacterial properties of the ligand and its metal(II) complexes on various microorganisms were also studied. SWISS-ADME online freeware was used to screen these compounds for drug-like action and pharmacokinetic research. Furthermore, UV absorption analyses and viscosity titrations were employed to test the efficacy of the synthesised metal complexes as DNA nucleases, and the results are consistent with an intercalative binding mechanism. The outcomes of molecular docking research on the COVID-19 virus and cancer DNA are fascinating.

**Keywords: Malonic acid, Intercalation DNA binding, Antimicrobial activity, *In silico*, Molecular docking.**

## INTRODUCTION

Anticancer medications often target DNA as their main intracellular target and their effectiveness is mediated through DNA binding. The design and discovery of new, more effective medications are fundamentally driven by this [1]. The field of coordination chemistry underwent a substantial upheaval once cisplatin was unintentionally discovered to be as anticancer drug. It is crucial to develop new cancer medicines with high cure rates and controllable adverse effects because cisplatin still has substantial negative effects. It expands the possibility for cross-disciplinary study fields and leads to the merging of medicinal chemistry and coordination chemistry [2-8].

Due to their increased stability and chelating characteristics, Schiff bases and related metal complexes are widely used in the catalytic and medicinal chemistry [9]. Similar to the above, due to the presence of N and O donor atoms, more focus has been placed on the synthesis of transition metal complexes with Schiff bases [10-12]. There have been numerous reports of Schiff base metal complexes with intriguing properties for biological and therapeutic action [13-15]. Schiff bases are important in coordination chemistry because they form stable complexes with the majority of transition metal ions [16,17]. During the synthesis of organic molecules, Schiff base reactions are useful for the creation of carbon-nitrogen bonds. Several physiologically relevant Schiff bases have been reported in the literature to have antimicrobial, antibacterial, antifungal, anti-inflammatory, anticonvulsant, anticancer and anti-HIV effects [18-22]. Because of their importance in facilitating interactions between DNA and metal complexes [23] and because they represent an advancement on our earlier study [24], the type of co-ligands used and the geometrical orientation of the synthesized complex are taken into account when developing the current work. The importance of the ligands in a metal complex has been shown by the experimental evidence presented in this work. Particularly, a number of chemical interactions, including electrostatic interaction, groove binding and intercalation, can allow various medicines and metal complexes

to interact with DNA. Regarding the planarity, donor sites and coordination geometry of the metal centre, among these modalities, binding to DNA through intercalation *via* planar ligands can also intercalate with adjacent base pairs of DNA [25,26]. The synthesis, characterization, DNA binding and antibacterial investigations of a series of new square planar complexes using malonic acid as including co-ligand are very interesting. The compounds are Schiff base complexes with central metal ions of Cu(II), Co(II), Ni(II) and Zn(II). The obtained results are useful for further study in the development and synthesis of effective antibacterial drugs as well as potent DNA probes, both of which are needed to satisfy the expectations of the researchers who are working to develop a successful medicine.

## EXPERIMENTAL

All the solvents and reagents used were of analytical agent supplied from Sigma-Aldrich, USA, whereas the metal(II) salts were purchased from E. Merck. All the organic solvents were distilled from appropriate drying agents immediately prior to use.

**Characterization:** Elemental analyses (C, H and N) were performed using a Perkin-Elmer 240C elemental analyzer. Attenuated total internal reflection (ATR) solid state Infrared spectra were performed on a Bruker TENOR 27 spectrometer using a KBr pellet in the range of 4000-400 $cm^{-1}$. $^1H$ NMR was recorded on a JEOL EX270, Bruker DPX 300, DPX 400 or AV 400 spectrometer using TMS ($SiMe_4$) as an internal reference. Absorption spectra were measured by using JASCO V-530 UV-VIS spectrophotometer at room temperature.

**Synthesis of metal(II) complexes:** The Cu(II), Ni(II), Co(II) and Zn(II) metal(II) chlorides were separately combined in an equimolar ratio with the Schiff base ligand (L), which was synthesized by reported method using *o*-phenylene diamine (0.755 g, 5 mmol) and 4-chlorobenzaldehyde (1.81 g, 10 mmol) [27]. The reaction mixture was dissolved and stirred in ethanol. The co-ligand (malonic acid, 0.520 g, 5 mmol) was then added and allowed to dissolve in an ethanolic solution. The finished product was reacted for 3 h in a 100 mL round bottom flask. It was then filtered off, washed with cold ethanol and petroleum ether and dried in a vacuum desiccator over anhydrous $CaCl_2$ (**Scheme-I**).

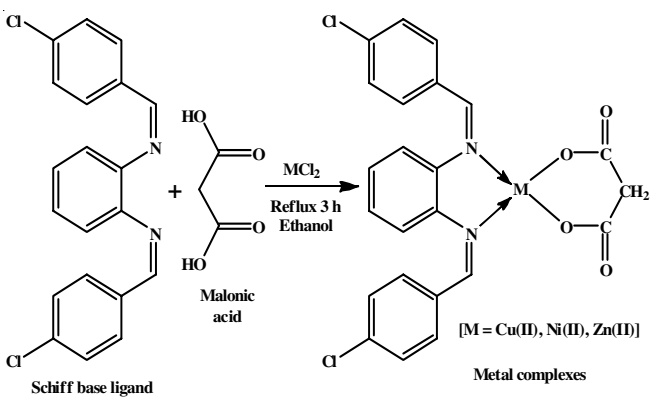


**Scheme-I:** Synthesis of Schiff base transition metal(II) complexes

**[CuL(MA)] (1):** Reddish brown, yield: 55%. Elemental anal. calcd. (found) % $C_{23}H_{18}N_2O_4Cl_2Cu$ (m.w. 520): C, 53.04 (52.85); H, 3.48 (3.28); Cl, 13.56 (13.36); N, 5.38 (5.17); Cu 12.20 (12.01). $\Lambda_m$ (mho $cm^2$ $mol^{-1}$): 13.2; Magnetic moment (B.M.) = 1.82.

**[ZnL(MA)] (2):** Brownish yellow, Yield: 54%. Elemental anal. calcd. (found) % $C_{23}H_{18}N_2O_4Cl_2Zn$ (m.w. 523): C, 52.85 (52.67); H, 3.47 (3.26); Cl, 13.57 (13.38); N, 5.36 (5.15); Zn, 12.51 (12.33). $\Lambda_m$ (mho $cm^2$ $mol^{-1}$): 10.1.

**[CoL(MA)] (3):** Violet solid, yield: 52%. Elemental anal. calcd. (found) % $C_{23}H_{18}N_2O_4Cl_2Co$ (m.w. 516): C, 53.51 (53.30); H, 3.51 (3.34); Cl, 13.74 (13.55); N, 5.43 (5.23); Co, 11.42 (11.21). $\Lambda_m$ (mho $cm^2$ $mol^{-1}$): 12.3; Magnetic moment (B.M.) = 3.83.

**[NiL(MA)] (4):** Yellowish solid, yield: 56.5%. Elemental anal. calcd. (found) % $C_{23}H_{18}N_2O_4Cl_2Ni$ (m.w. 516): C, 53.54 (53.35); H, 3.52 (3.33); Cl, 13.74 (13.56); N, 5.43 (5.24); Ni, 11.37 (11.18). $\Lambda_m$ (mho $cm^2$ $mol^{-1}$): 11.4.

**DNA binding studies:** The interactions of the synthesized metal complexes with deoxyribonucleic acid from calf thymus (*ct*-DNA) were studied in 5 mM Tris-HCl/50mM NaCl buffer solution at pH 7.2 [28,29]. In this experiment, the concentration of *ct*-DNA was varied between 0-10 μM by keeping the total volume of the synthesized compounds constant (3 mL). After each addition of *ct*-DNA to the complex, the resulting solution was allowed to equilibrate at 25 ºC for 5 min followed by recording of the absorption spectrum. The binding constant values ($k_b$) were calculated from the spectroscopic titration data by the plot between [DNA] /($\varepsilon_a - \varepsilon_f$) and [DNA].

Viscosity measurements were carried out on an Ostwald's micro-viscometer, immersed in a thermostatic water bath at constant temperature (30 ± 1 ºC). In addition, stopwatch was used to measure the fluidity times at varied concentrations of the as prepared Schiff base imine-metal complexes from 10 to 60 μM, making the DNA concentration unchanged at 50 μM [30]. The measured data were plotted as $(\eta/\eta_o)^{1/3}$ *vs.* [complex/DNA], where $\eta$ is the viscosity of DNA alone and $\eta_o$ is the viscosity of DNA in the presence of synthesized compound.

**Molecular docking studies:** Molecular docking studies were carried out using the Hex 8.00 on windows 10 professional workstation. When docking was performed with default settings, it revealed a number of possible conformations and orientations for the inhibitors at the binding site [31]. The crystal 3D structure of SARS-CoV-2COVID-19 (SARS-CoV-2) $M^{pro}$ (PDB ID: 6M71) collected from online Protein Data Bank (PDB) and used as receptor protein. The water removed from chain A of receptor protein by Argus lab.exe software package and saved in PDB format [31,32]. All the compounds were optimized using Avogadro version 1.2. Hex 8.00 was used, headed for screen potential drugs with molecular docking by the structural protein and non-structural protein site of new corona viruses and the study was constructed to molecular docking without validation through MD simulators. Interaction with main protease may play a key role in fighting against viruses. The results obtained from docking were visualized through Discovery studio.

**Antimicrobial activity:** All the newly synthesized compounds were tested for their antibacterial activities against Gram-positive bacteria *Staphylococcus aureus*, *Staphylococcus typhi*

and *Bacillus subtilis* and Gram-negative bacteria *Eschrichia coli* and *Pseudomonas vulgaris* and antifungal activity against *Aspergillus niger*, *Aspergillus flavusi*, *Curuvulaic lunata*, *Rhizoctonia bataticola* and *Candida albicans*. The method used to evaluate the antimicrobial activity was Broth dilution method. It is one of the non-automated *in vitro* susceptibility tests [33]. The minimum inhibitory concentration (MIC) of the control organism was read to check the accuracy of the drug concentrations. The lowest concentration inhibiting growth of the organism was recorded as the MIC. The MIC values of the newly synthesized compounds were compared with the standard drugs ciprofloxacin and fluconazole [34].

***In vitro* free radical scavenger activity using DPPH assay:** All the synthesized metal complexes in $10^{-4}$ mM and the standard vitamin C (0.1 mM) were mixed with DPPH (0.1 mM) in ethanolic solution. After 20 min incubation at room temperature, the absorbance at 517 nm was measured. The inhibitory percentage of DPPH (antioxidant activity) was calculated as follows [35]:

$$\text{Activity (\%)} = \frac{\text{Abs. of control} - \text{Abs. of sample}}{\text{Abs. of control}} \times 100$$

## RESULTS AND DISCUSSION

**IR studies:** The IR spectra of the metal(II) complexes are displayed in Fig. 1. In comparison to the ligand, all of the synthesized metal(II) complexes (1587-1578 $cm^{-1}$ have lower ν(-CH=N-) values due to the imine group double bond nature (1598 $cm^{-1}$) [36]. The extra bands in complexes at 1633, 1354 and 832 $cm^{-1}$ may be caused by the carboxylate moiety's vibrations. This reveals that malonic acid has two moieties and that the two accessible monodentate carboxylate groups enable it to connect with metal(II) centres. These mixed ligand complexes displayed the carboxylate moiety's stretching vibration at 1678-1673 $cm^{-1}$. In contrast, the high value of the malonic group enables the C=O group to unshare in coordination with the metal ion, acting as a dianionic bidentate ligand. The development of the metal oxygen bond ν(M-O) in complexes in the

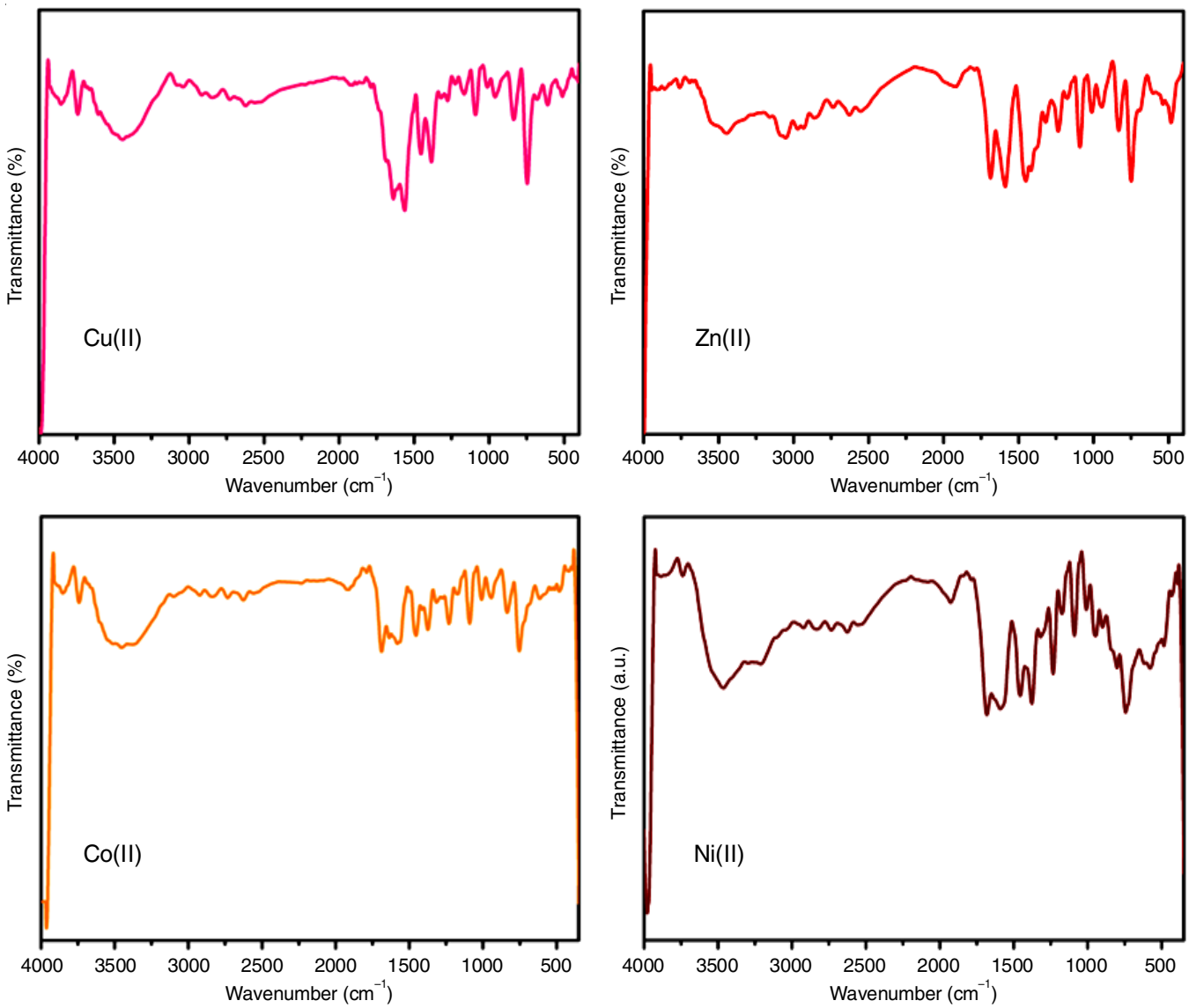


Fig. 1. FT-IR spectra of Cu(II), Zn(II), Co(II) and Ni(II) complexes

569-557 $cm^{-1}$ range provides additional support. The new band seen in complexes at 471-443 $cm^{-1}$ region is a indication of metal-nitrogen (M-N) bonding.

**Electromagnetic studies:** The electronic absorbance spectra of Schiff base ligand-metal(II) complexes in DMSO solution are displayed in Fig. 2. The electronic spectra and magnetic moment data of the metal(II) complexes were used to derive the geometry. The broad band observed at 555 nm, visible in the electronic spectrum of Cu(II) complex, is associated with the $^2B_{1g} \rightarrow {}^2A_{1g}$ transition. The Cu(II) complex was identified as having a square planar shape, based on the electronic spectral data. The magnetic moment of copper(II) complex is 1.84 B.M. A band at 575 nm in Ni(II) complex exhibits a four-coordinate square-planer structure as a result of the $^2A_{1g} \rightarrow {}^2A_{2g}$ transition, while a broad band at 583 nm in the electronic spectrum of Co(II) complex, associated with the $^4A_2(F) \rightarrow {}^4T_{1g}$ transition, is suggestive of a square planar structure. Three unpaired electrons in the Co(II) complex are demonstrated to have a 3.85 B.M. magnetic moment [37]. Band at 351 nm in the electronic absorption spectrum of diamagnetic Zn(II) complex was attributed to intraligand charge-transfer transition [38].

**NMR studies:** The multiplet peaks of Zn(II) complex appear between δ 6.9 and 7.9 ppm show that the generated molecules include an aromatic group. The imine peak for the ligand is appeared at 9.55 ppm and moved upfield to δ 8.19 ppm in the complex. Similar peaks at δ 111-156 ppm may be identified in the $^{13}C$ NMR spectra of the aromatic carbons in the ligand. Furthermore, a shift from 171 ppm to 169 ppm is seen in the upfield position of the C=N carbons in the ligand to Zn(II) complex. The observed upfield shift which suggests the C=N involvement in the complexation.

**Mass studies:** Molecular ion peaks and ESI-mass spectra of the synthesized Schiff base ligand and its metal(II) complexes provide independent confirmation of the proposed structures. The $[M^+]$ peak for the ligand is observed in the mass spectrum at *m/z* 354, which corresponds to $[C_{20}H_{14}N_2Cl_2]$ species. Also, in the visible spectrum, the fragments $[C_{20}H_{15}N_2Cl]$, $[C_{20}H_{16}N_2]$, $[C_{14}H_{12}N_2]$ and $[C_8H_8N_2]$ are observed at *m/z* 319, 284, 214 and 132, respectively [27]. The [M+] peak at *m/z* 516 is seen in the mass spectrum of Zn(II) complex. Its molecular formula is found to be $[C_{23}H_{18}Cl_2N_2O_4Zn]$ which has the *m/z* value 516. The stable species $[C_{20}H_{16}N_2Cl_2]$ is shown by the strongest peak (base beak) at *m/z* 355. The complex stoichiometry of the [ZnL(MA)], is confirmed by the *m/z* values of ligand and its metal(II) complex components. The observed peaks and their formulae as derived from micro-analytical data are in good accord.

### *In vitro* analysis

**DNA binding:** The absorption spectra of the metal(II) complexes in the presence of DNA result hypochromism [39]. Therefore, intercalation can be used to describe the binding mode. However, the ability of the metal(II) complexes to bind DNA is significantly influenced by the metal ions (Table-1). The order of binding strength of the synthesized complexes is as follows: [CuL(MA)] > [ZnL(MA)] > [NiL(MA)] > [CoL-(MA)]. In contrast to the other complexes, complex **1** exhibits severe hypochromism and a mild red shift, demonstrating its stronger DNA binding affinity. In every case, the complexes have higher intrinsic binding constant values, representing the state-of-the-art in cancer therapy (Fig. 3) [40]. According to the findings, the ligand itself performs weak intercalation compared to complexes that perform high intercalation. These findings imply that the ability to bind DNA can be significantly enhanced by intercalative ligands with a prolonged aromatic plane and good conjugation action [41].

TABLE-1
ELECTRONIC ABSORPTION SPECTRAL PROPERTIES OF Cu(II) AND Zn(II) COMPLEXES

| Compound | $\lambda_{max}$ | | Δλ (nm) | H%[a] | $K_b \times 10^4$ $(M^{-1})$[b] |
|---|---|---|---|---|---|
| | Free | Bound | | | |
| [CuL(MA)] | 430 | 424 | 6 | 1.39 | 4.7 |
| [ZnL(MA)] | 435 | 428 | 7 | 1.60 | 3.5 |
| [NiL(MA)] | 424 | 419 | 5 | 1.17 | 3.1 |
| [CoL(MA)] | 429 | 422 | 7 | 1.63 | 2.9 |

[a]$H\% = [A_{free} - A_{bound})/A_{free}] \times 100$; [b]$K_b$ = Intrinsic DNA binding constant determined from the UV–Vis absorption spectral titration.

**Viscosity measurements:** A binding model cannot be determined using optical or photophysical techniques, which are typically employed to analyze the binding of ligands and their complexes to DNA. In general, optical or photophysical probes offer necessary but insufficient information to back up an intercalative binding model. When different amounts of the substance were added to the DNA solution for intercalation mode, the viscosity of the solution generally increases. The

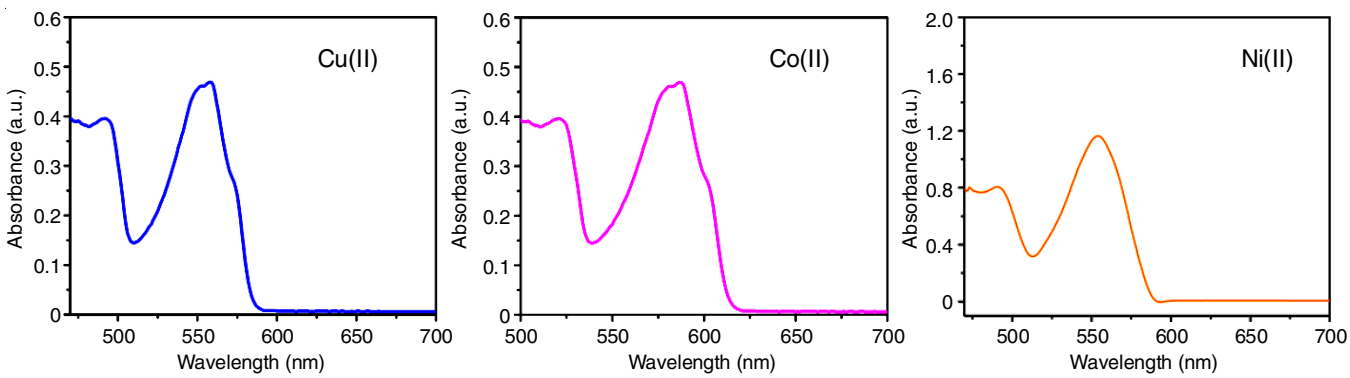


Fig. 2. Electronic absorption spectra of Cu(II), Co(II) and Ni(II) complexes

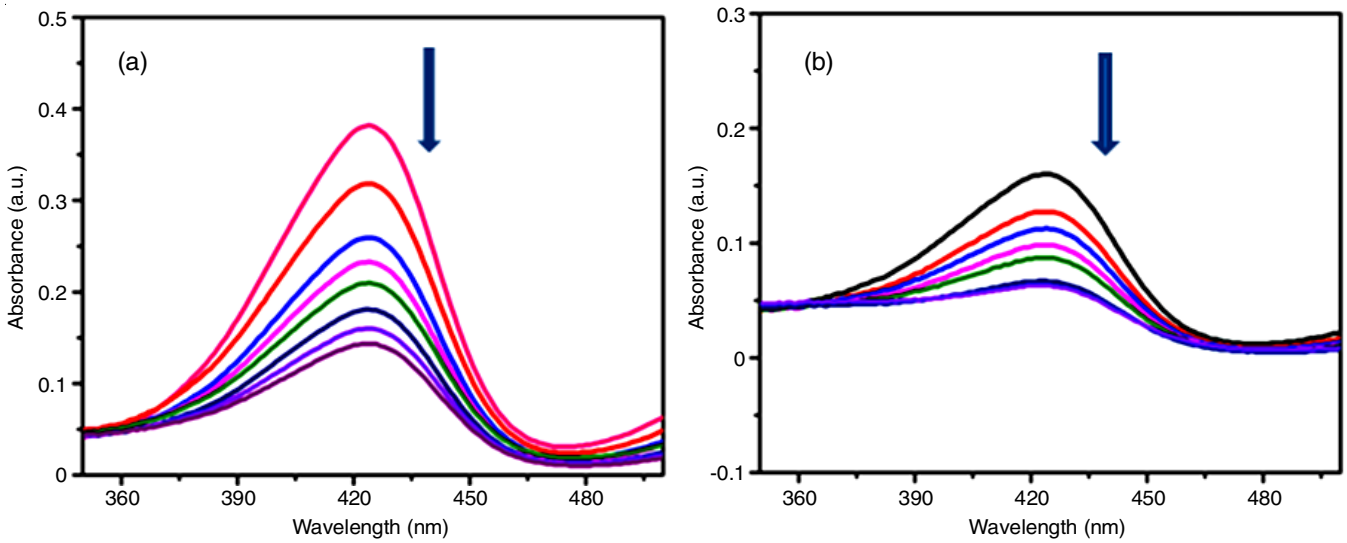


Fig. 3. (a) Absorption spectrum of $10^{-3}$ M DMSO solution of complex **1** in buffer (pH =7.2) at 25 °C in presence of increasing amount of DNA, (b) Absorption spectrum of $10^{-3}$ M DMSO solution of complex **2** in buffer (pH =7.2) at 25°C in presence of increasing amount of DNA. Arrow indicates the changes in absorbance upon increasing the DNA concentration

results of the viscosity studies conclusively show that all the complexes were capable of intercalating between nearby DNA base pairs, lengthening the helix and increasing DNA viscosity in the process (Fig. 4). Similar to the behaviour of ethidium bromide, the relative viscosity of DNA increases slightly as the number of metal(II) complexes increases. When the concentration of the complexes increases, a stronger intercalation might occur, increasing the viscosity of the DNA. It is inferring that all complexes interact with DNA in an intercalation way from spectroscopic study and viscosity measurements [42,43].

**Antimicrobial studies:** Using the broth micro-dilution method, the synthesized metal(II) complexes **1-4** were evaluated *in vitro* for antimicrobial activity against 5 bacterial and 5 fungal pathogens (Table-2). Their effectiveness was assessed in comparison to common medications ciprofloxacin and fluconazole. Based on the overtone concept [44] and Tweedy's chelation theory [45] the cause can be identified. The activity was found in the following order: [CuL(MA)] > [ZnL(MA)] > [NiL(MA)] > [CoL(MA)]. It is clear from the order of activity that the co-ligands are crucial to biological activity. According to the antimicrobial data, all of the synthesized metal(II) complexes exhibit higher antibacterial and antifungal activity than the parent Schiff base ligand [46].

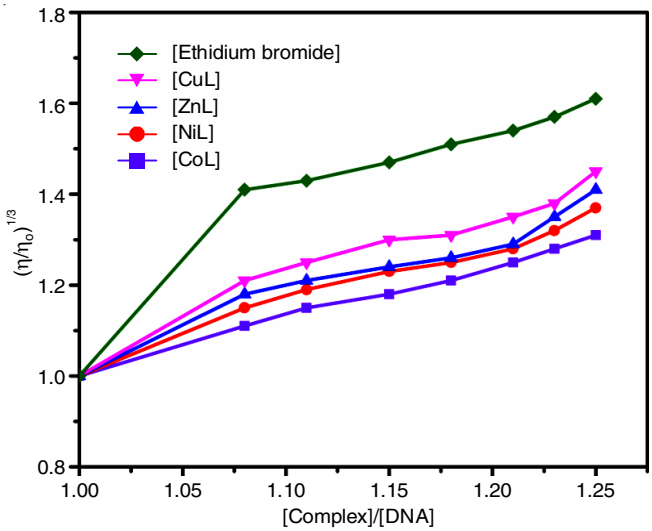


Fig. 4. Plot of relative viscosity $(\eta/\eta_o)^{1/3}$ *vs.* [complex]/[DNA]

**Antioxidant studies:** Schiff base ligand and its metal(II) complexes were examined for antioxidant activity using the DPPH assay (free radical scavenging activity). A visible component of DPPH has substantial absorbance at 517 nm and this

TABLE-2
MINIMUM INHIBITORY CONCENTRATION OF THE SYNTHESIZED METAL(II) COMPLEXES AGAINST THE GROWTH OF BACTERIA AND FUNGI (?M)

| Compound | MIC values (× $10^4$ μM) SEM = ± 1.2 | | | | | | | | | |
|---|---|---|---|---|---|---|---|---|---|---|
| | Bacteria | | | | | Fungi | | | | |
| | *S. aureus* | *P. vulgaris* | *E. coli* | *B. subtilis* | *S. typhi* | *A. niger* | *A. flavusi* | *C. lunata* | *R. bataticola* | *C. albicans* |
| [CuL(MA)] | 4.1 | 4.6 | 3.7 | 3.9 | 4.8 | 4.9 | 4.1 | 5.3 | 5.1 | 5.9 |
| [ZnL(MA)] | 4.9 | 5.1 | 4.5 | 4.7 | 5.4 | 5.8 | 5.2 | 6.3 | 7.1 | 6.3 |
| [NiL(MA)] | 5.1 | 5.5 | 4.6 | 4.9 | 5.9 | 6.5 | 5.9 | 6.9 | 7.5 | 7.8 |
| [CoL(MA)] | 5.8 | 6.1 | 5.2 | 5.5 | 6.3 | 6.9 | 6.4 | 7.3 | 7.9 | 8.3 |
| Ciprofloxacin | 1.8 | 1.7 | 2.1 | 1.9 | 2.6 | – | – | – | – | – |
| Fluconazole | – | – | – | – | – | 1.1 | 1.4 | 1.1 | 1.3 | 1.9 |

absorbance will decrease when metal(II) complexes are introduced. The decolorization of the DPPH solution was caused by the stable DPPH free radical being reduced and converted into 1,1-diphenyl-2-picrylhydrazine by acquiring an electron from an antioxidant molecule. Copper(II) complex has greater antioxidant activity than other metal(II) complexes but less antioxidant activity than ascorbic acid (Table-3). These findings clearly show that copper complex has higher antioxidant action [47,48].

## ADMET properties

***In silico* examination:** A SWISS-ADME online programme was used to examine the pharmacokinetic behaviours of the synthesized compounds and the results are shown in Table-4. These outcomes can be evaluated using five Lipinski's rules [49,50]. The total surface area of all polar oxygen and nitrogen atoms is known as the total polar surface area (TPSA) (including their attached hydrogen atom). For the effective transfer of the produced chemicals inside the gut and BBB, the optimal TPSA values are fewer than 140 Å. Table-4 shows the pharmacokinetic activities results of the synthesized metal(II) complexes.

TABLE-3
PERCENTAGE OF ANTIOXIDANT ACTIVITY OF METAL COMPLEXES

| Compound | Concentration (µg/mL) | | | |
|---|---|---|---|---|
| | 10 | 20 | 30 | 40 |
| [CuL(MA)] | 71.24 | 77.28 | 85.35 | 89.13 |
| [ZnL(MA)] | 68.23 | 74.19 | 81.25 | 86.27 |
| [NiL(MA)] | 66.13 | 71.25 | 77.36 | 81.36 |
| [CoL(MA)] | 64.18 | 69.27 | 72.36 | 80.38 |
| Vitamin C | 80.78 | 86.37 | 89.21 | 93.38 |

**Molecular docking studies:** The Discovery Studio Visualizer 4.0 programme was used to eliminate the water that was present in the SARS-CoV-2 receptor structure after it was extracted from the PDB. Hex 8.0 software was used to perform the molecular docking in the current investigation. All the synthesized compounds firmly attach to receptors since their amino acid constituents bind the hydrogen bonds [51,52]. Table-5 lists the amino acids that bind with synthetic compounds along with the docking scores. The active sites of the receptors were primarily composed of the amino acids PRO111 (Figs. 5 and 6). Due to its lowest docking score value of -392.00 KJ $mol^{-1}$ among all the compounds, copper(II) complex conducts a more efficient docking process with the receptor. This study provides evidence that these synthesized compounds suppress the SAR CoV-2 inhibitory activity [53].

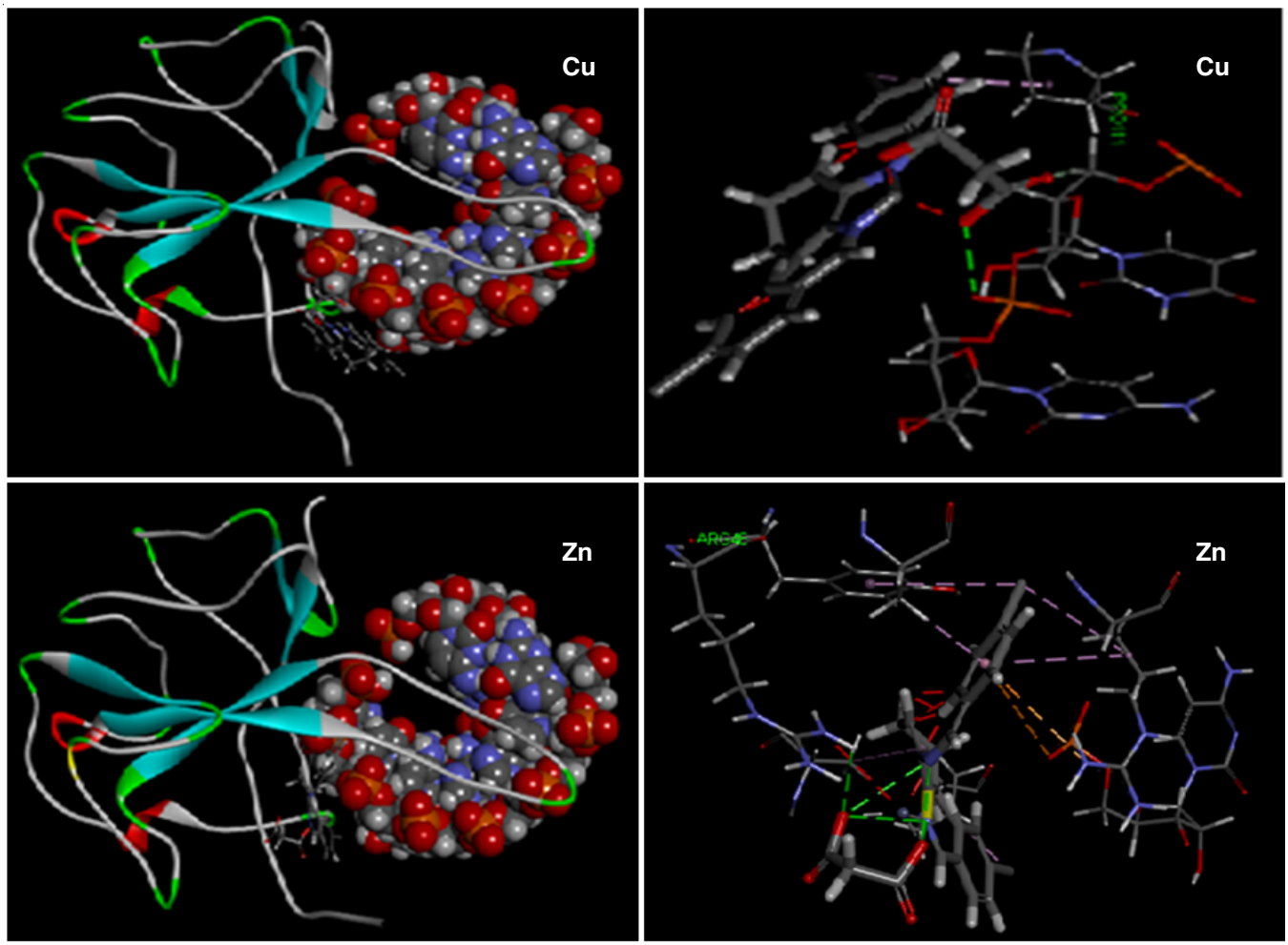


Fig. 5. Molecular docking SARS Cov receptor 7ACS of the ligand. Three dimension (3D) binding interaction of Cu(II) and Zn(II) complexes with DNA (SARS Cov receptor 7ACS)

TABLE-4
PREDICTION OF *in silico* ADMET PROPERTIES OF THE SYNTHESIZED COMPOUNDS

| Compound | Physico-chemical properties | | | | | | Bio activity score |
|---|---|---|---|---|---|---|---|
| | TPSA (Å²) | Molar refractivity | Synthetic accessibility | Number of H-acceptors | Number of H-donors | Number of rotatable bonds | |
| [CuL(MA)] | 87.32 | 151.53 | 4.62 | 4 | 0 | 4 | 0.55 |
| [ZnL(MA)] | 83.32 | 151.53 | 4.43 | 4 | 0 | 2 | 0.55 |
| [NiL(MA)] | 83.32 | 151.53 | 4.27 | 4 | 0 | 2 | 0.55 |
| [CoL(MA)] | 83.32 | 151.53 | 4.44 | 4 | 0 | 2 | 0.55 |

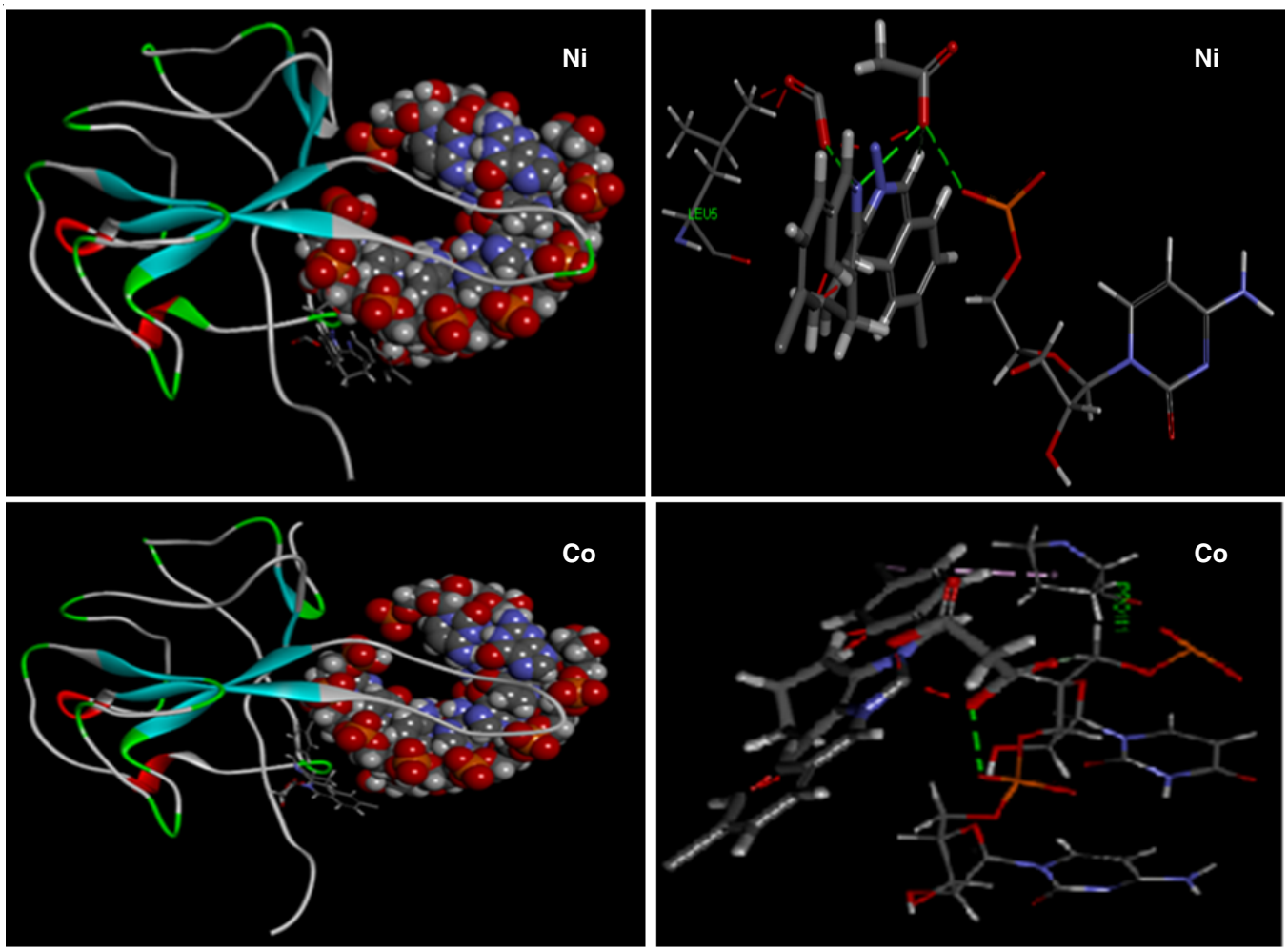


Fig. 6. Three dimension (3D) binding interaction of Ni(II) and Co(II) complexes with DNA (SARS Cov receptor 7ACS)

TABLE-5
DOCKING SCORES FOR SYNTHESIZED COMPOUNDS WITH 7AEH PROTEASE OF SARS-CoV-2 TARGET AND THEIR INTERACTING AMINO ACIDS

| Compounds | Binding score (KJ $mol^{-1}$) | Interacting amino acid |
|---|---|---|
| [CuL(MA)] | -392.00 | PRO111 |
| [ZnL(MA)] | -381.64 | ARG48 |
| [NiL(MA)] | -374.89 | LEU5 |
| [CoL(MA)] | -369.37 | ASN8, ALA10, TYR69, ASN7 |

## Conclusion

Four mixed ligands transition metal(II) complexes have been synthesized in this study and characterized by IR, UV-Vis, ESI-mass, $^{13}C$ NMR, $^{1}H$ NMR and microanalytical data, which corroborated the equimolar (1:1:1 (M:L:coligand)) stoichiometry of Cu(II), Co(II), Ni(II) and Zn(II) complexes that adopt square planar geometry. Among the synthesized complexes, Cu(II) complex possesses higher antibacterial and antimicrobial activity than other metal(II) complexes. From the results, it was observed that chelation plays in the development of effective antibacterial activities. *In vitro* research with antioxidants has been used to investigate how efficient complexes are as a kind of protection against the DPPH free radical generator. The findings indicate that the complexes intercalatively bind with DNA and a molecular docking analysis provides additional evidence to confirm these results.

## ACKNOWLEDGEMENTS

We express our sincere thanks to the Head, Principal and College Managing Board for providing the research facilities and their constant encouragement. M.Nazeer thanks Sri Kaliswari College (Autonomous) Managing Board, Principal and Head of the Department of Chemistry, Sivakasi for their moral support.

## CONFLICT OF INTEREST

The authors declare that there is no conflict of interests regarding the publication of this article.

## REFERENCES

1. G.J. Kelloff, *Adv. Cancer Res.*, **78**, 199 (1999); https://doi.org/10.1016/S0065-230X(08)61026-X
2. S. Jana, R.C. Santra, A. Frontera, M.G.B. Drew, J. Ortega-Castro, D. Fernandez, S. Das and S. Chattopadhyay, *ChemistrySelect*, **1**, 448 (2016); https://doi.org/10.1002/slct.201500018
3. C.G. Hartinger and P.J. Dyson, *Chem. Soc. Rev.*, **38**, 391 (2009); https://doi.org/10.1039/B707077M
4 G.S. Smith and B. Therrien, *Dalton Trans.*, **40**, 10793 (2011); https://doi.org/10.1039/c1dt11007a
5 N.P.E. Barry and P.J. Sadler, *Chem. Commun.*, **49**, 5106 (2013); https://doi.org/10.1039/c3cc41143e
6. P. Govender, B. Therrien and G.S. Smith, *Eur. J. Inorg. Chem.*, 2853 (2012); https://doi.org/10.1002/ejic.201200161
7. U. Jungwirth, C.R. Kowol, B.K. Keppler, C.G. Hartinger, W. Berger and P. Heffeter, *Antioxid. Redox Signal.*, **15**, 1085 (2011); https://doi.org/10.1089/ars.2010.3663
8. C.H. Wang, W.C. Shih, H.C. Chang, Y.Y. Kuo, W.C. Hung, T.G. Ong and W.S. Li, *J. Med. Chem.*, **54**, 5245 (2011); https://doi.org/10.1021/jm101096x
9. S. Kundu, A.K. Pramanik, A.S. Mondal and T.K. Mondal, *J. Mol. Struct.*, **1116**, 1 (2016); https://doi.org/10.1016/j.molstruc.2016.03.013
10. K. Buldurun, N. Turan, A. Savci and N. Çolak, *J. Saudi Chem. Soc.*, **23**, 205 (2019); https://doi.org/10.1016/j.jscs.2018.06.002
11. A. Gölcü, M. Tümer, H. Demirelli and R.A. Wheatley, *Inorg. Chim. Acta*, **358**, 1785 (2005); https://doi.org/10.1016/j.ica.2004.11.026
12. P. Krishnamoorthy, P. Sathyadevi, K. Senthilkumar, P.T. Muthiah, R. Ramesh and N. Dharmaraj, *Inorg. Chem. Commun.*, **14**, 1318 (2011); https://doi.org/10.1016/j.inoche.2011.05.004
13. R.V. Sakthivel, P. Sankudevan, P. Vennila, G. Venkatesh, S. Kaya and G. Serdaroğlu, *J. Mol. Struct.*, **1233**, 130097 (2021); https://doi.org/10.1016/j.molstruc.2021.130097
14. A.K. Patra, M. Nethaji and A.R. Chakravarty, *J. Inorg. Biochem.*, **101**, 233 (2007); https://doi.org/10.1016/j.jinorgbio.2006.09.018
15. A. Silvestri, G. Barone, G. Ruisi, M.T. Lo Giudice and S.J. Tumminello, *J. Inorg. Biochem.*, **98**, 589 (2004); https://doi.org/10.1016/j.jinorgbio.2004.01.010
16. M. Navarro, E.J. Cisneros-Fajardo, A. Sierralta, M. Fernandez-Mestre, P. Silva, D. Arrieche and E. Marchan, *J. Biol. Inorg. Chem.*, **8**, 401 (2003); https://doi.org/10.1007/s00775-002-0427-2
17. S.N. Pandeya, D. Sriram, G. Nath and E. De Clercq, *Pharm. Acta Helv.*, **74**, 11 (1999); https://doi.org/10.1016/S0031-6865(99)00010-2
18. S.N. Pandeya, D. Sriram, G. Nath and E. de Clercq, *Arzneimittelforschung*, **50**, 55 (2000); https://doi.org/10.1055/s-0031-1300164
19. W.M. Singh and B.C. Dash, *Pesticides*, **22**, 33 (1988).
20. J.L. Kelley, J.A. Linn, D.D. Bankston, C.J. Burchall, F.E. Soroko and B.R. Cooper, *J. Med. Chem.*, **38**, 3676 (1995); https://doi.org/10.1021/jm00018a029
21. G. Turan-Zitouni, Z.A. Kaplancikli, A. Özdemir, P. Chevallet, H.B. Kandilci and B. Gümüsel, *Arch. Pharm.*, **340**, 586 (2007); https://doi.org/10.1002/ardp.200700134
22. M.T.H. Tarafder, A. Kasbollah, N. Saravanan, K.A. Crouse, A.M. Ali and K. Tin Oo, *J. Biochem. Mol. Biol. Biophys.*, **6**, 85 (2002); https://doi.org/10.1080/10258140290027207
23. S.T. Chew, K.M. Lo, S.K. Lee, M.P. Heng, W.Y. Teoh, K.S. Sim and K.W. Tan, *Eur. J. Med. Chem.*, **76**, 397 (2014); https://doi.org/10.1016/j.ejmech.2014.02.049
24. N. Raman and N. Pravin, *Eur. J. Med. Chem.*, **80**, 57 (2014); https://doi.org/10.1016/j.ejmech.2014.04.032
25. G. Psomas, *J. Inorg. Biochem.*, **102**, 1798 (2008); https://doi.org/10.1016/j.jinorgbio.2008.05.012
26. X. Qiao, Z.-Y. Ma, C.-Z. Xie, F. Xue, Y.-W. Zhang, J.-Y. Xu, Z.-Y. Qiang, J.-S. Lou, G.-J. Chen and S.-P. Yan, *J. Inorg. Biochem.*, **105**, 728 (2011); https://doi.org/10.1016/j.jinorgbio.2011.01.004
27. N.M. Nasar, M. Samuel, P. Jayaraman, F.S. Sheela and N. Raman, *Asian J. Chem.*, **35**, 639 (2023); https://doi.org/10.14233/ajchem.2023.27565
28. F.T. Elmali, *J. Mol. Struct*., **1261**, 132900 (2022); https://doi.org/10.1016/j.molstruc.2022.132900
29. E. Oguzcan, Z. Koksal, T. Taskin-Tok, A. Uzgoren-Baran and N. Akbay, *Spectrochim. Acta Part A: Mol. Biomol. Spectrosc.*, **270**, 120787 (2022); https://doi.org/10.1016/j.saa.2021.120787
30. S.V. Aswathy, I.H. Joe and K.B. Rameshkumar, *J. Mol. Struct*., **1263**, 133152 (2022); https://doi.org/10.1016/j.molstruc.2022.133152
31. M.N. Uddin, M.S. Amin, M.S. Rahman, S. Khandaker, W. Shumi, M.A. Rahman and S.M. Rahman, *Appl. Organomet. Chem*., **35**, e6067 (2021); https://doi.org/10.1002/aoc.6067
32. A. Senocak, N.A. Tas, P. Taslimi, B. Tüzün, A. Aydin and A. Karadag, *J. Biochem. Mol. Toxicol*., **36**, e22969 (2022); https://doi.org/10.1002/jbt.22969
33. M. Balouiri, M. Sadiki and S.K. Ibnsouda, *J. Pharm. Anal.*, **6**, 71 (2016); https://doi.org/10.1016/j.jpha.2015.11.005
34. M. Gupta, B.K. Sarma, S. Chandra, S. Gupta and S. Singhal, *Int. J. Therap. Appl*., **35**, 29 (2018).
35. Q.H. Tran and T.T. Doan, *New J. Chem.,* **44**, 13036 (2020); https://doi.org/10.1039/D0NJ01159B
36. K. Nakamato, Infrared and Raman Spectra of Inorganic and Coordination Compounds, Wiley: New York, Edn. 4 (1986).
37. M. Shakir, A. Abbasi, A.U. Khan and S.N. Khan, *Spectrochim. Acta A Mol. Biomol. Spectrosc.*, **78**, 29 (2011); https://doi.org/10.1016/j.saa.2010.02.034
38. N. Shahabadi, S. Kashanian and F. Darabi, *Eur. J. Med. Chem.*, **45**, 4239 (2010); https://doi.org/10.1016/j.ejmech.2010.06.020
39. J.Z. Wu, L. Yuan and J.F. Wu, *J. Inorg. Biochem.*, **99**, 2211 (2005); https://doi.org/10.1016/j.jinorgbio.2005.08.002
40. C.N. N'soukpoé-Kossi, C. Descôteaux, É. Asselin, H.-A. Tajmir-Riahi and G. Bérubé, *DNA Cell Biol.*, **27**, 101 (2008); https://doi.org/10.1089/dna.2007.0669
41. S. Satyanarayana, J.C. Dabrowiak and J.B. Chaires, *Biochemistry*, **32**, 2573 (1993); https://doi.org/10.1021/bi00061a015
42. S. Satyanarayana, J.C. Dabrowiak and J.B. Chaires, *Biochemistry*, **31**, 9319 (1992); https://doi.org/10.1021/bi00154a001
43. S. Packianathan, G. Kumaravel and N. Raman, *Appl. Organomet. Chem.*, **31**, e3577 (2017); https://doi.org/10.1002/aoc.3577
44. Y. Anjaneyulu and R.P. Rao, *Synth. React. Inorg. Met.-Org. Chem.*, **16**, 257 (1986); https://doi.org/10.1080/00945718608057530
45. N.N. Al-Mohammed, Y. Alias, Z. Abdullah, R.M. Shakir, E.M. Taha and A.A. Hamid, *Molecules*, **18**, 11978 (2013); https://doi.org/10.3390/molecules181011978

46. R. Taherlo and M. Salehi, *Inorg. Chim. Acta*, **418**, 180 (2014); https://doi.org/10.1016/j.ica.2014.04.028
47. S. Daravath, A. Rambabu, N. Vamsikrishna, N. Ganji and S. Raj, *J. Coord. Chem.*, **72**, 1973 (2019); https://doi.org/10.1080/00958972.2019.1634263
48. K.S. Abou-Melha, G.A. Al-Hazmi, I. Althagafi, A. Alharbi, F. Shaaban, N.M. El-Metwaly, M.A. El-Bindary and M.A. El-Bindary, *J. Mol. Liq.*, **334**, 116498 (2021); https://doi.org/10.1016/j.molliq.2021.116498
49. B. Mohan and M. Choudhary, *J. Mol. Struct.*, **1246**, 131246 (2021); https://doi.org/10.1016/j.molstruc.2021.131246
50. M. Samuel, R. Rajasekar, P. Jeyaraman, S. Muthusamy, V. Muniyandi and N. Raman, *Inorg. Chim. Acta*, **533**, 120783 (2022); https://doi.org/10.1016/j.ica.2021.120783
51. R. Reshma, R. Selwin Joseyphus, D. Arish, R.J. Reshmi Jaya and J. Johnson, *J. Biomol. Struct. Dyn.*, **40**, 8602 (2022); https://doi.org/10.1080/07391102.2021.1914171
52. J. Porkodi and N. Raman, *Appl. Organomet. Chem.*, **32**, e4030 (2018); https://doi.org/10.1002/aoc.4030
53. S. Michael, P. Jeyaraman, B. Marimuthu, R. Rajasekar, R. Thanasamy, K.A. Kumar and N. Raman, *J. Mol. Struct.*, **1279**, 134987 (2023); https://doi.org/10.1016/j.molstruc.2023.134987